Front. Phys. China (2006) 3: 323－333
DOI 10.1007/s11467-006-0021-0

REVIEW ARTICLE

**ZHANG Yan-feng, LI Shao-chun, MA Xu-cun,
JIA Jin-feng, XUE Qi-kun**

Quantum oscillations in Pb/Si (111) heterostructure system

Abstract This paper summarizes our recent work on the study of quantum size effects (QSE) and novel physical properties of the Pb/Si (111) heterostructure. Two different types of samples were investigated. One is wedge-shaped Pb islands, and the other is atomically flat Pb thin films. With scanning tunneling microscopy (STM) manipulation, we observed an intriguing morphology dynamics of the islands that swings between two extreme energy states, like that in a classical pendulum. We show that the dynamics is a result of the competition between the QSE and the classical step free energy minimizing effect. For the second type of the samples, the QSE is studied in terms of thickness-dependent film stability, electronic structure and physical properties by using STM, angle-resolved photoemission spectroscopy (ARPES) and transport measurement. The results consistently reveal the formation of quantum well states (QWS) due to electron confinement in the films. This size effect could greatly modify the electronic structure near the Fermi level and lead to quantum oscillations in superconductivity, electron-phonon coupling and thermal expansion. The work unambiguously demonstrates the possibility of quantum engineering of physical properties of thin films by exploiting well-controlled and thickness-dependent QSE.

Keywords quantum wells, scanning tunnelling microscopy, photoemission, thin films, physical properties

PACS numbers 73.21.Fg, 68.37.Ef, 79.60.-i, 79.60.Dp, 96.15.Pf

ZHANG Yan-feng, LI Shao-chun, MA Xu-cun, JIA Jin-feng,
XUE Qi-kun (✉)
Institute of Physics, Chinese Academy of Science,
Beijing 100080, China
E-mail: qkxue@aphy.iphy.ac.cn

XUE Qi-kun
Department of Physics, Tsinghua Univeristy, Beijing 100084, China

Received April 17, 2006

1 Introduction

Low dimensional nanostructures such as quantum wells, quantum wires and quantum dots with their characteristic scale comparable to the Fermi electron wavelength (λ_F) have attracted much attention recently. Many novel physical properties that differ from that of the bulk state can be expected due to strong quantum confinement of electron motion in these systems. For two dimensional systems, electrons confined in the normal direction of the film surface are quantized into the well-known QWS with discrete energy levels [1–3], which has been proven to greatly modulate the electronic density of states near the Fermi level (E_F), thus significantly affect the physical and chemical properties of the system. Such kind of quantum confinement can be achieved in thin films grown on semiconductor or insulator substrates where the conduction electrons are restricted within a potential well bounded by the vacuum barrier and the energy band gap of the substrate (or wave vector-dependent relative gap in the case of a metal).

Because the λ_F in Pb is nearly four times of the atomic plane spacing (a_0) along the (111) crystallographic direction, namely $\lambda_F \approx 4a_0$, the Pb thin film proves to be an ideal system for the study of QSE: film thickness variation by one atomic-layer can cause significant change in the electronic structure and physical properties [4–10]. Interference patterns of electron waves were observed in the wedge-shaped Pb islands on Si (111) [4], and scanning tunneling spectroscopy (STS) measurement revealed its quantum origin. Several groups studied the novel stability of Pb islands, where magic heights of the islands were identified by STM/STS [5]. In the case of atomically flat Pb films, investigation on the electronic structure by ARPES reveals the significance of QSE [10, 11]. However, most of the studies are limited to a relatively small thickness regime (<10 ML). For thicker films, there is an uncertainty in film uniformity as evidenced by the lack of a ~2 monolayer (ML) oscillatory period in the density of states [12, 13]. Because of the very short λ_F (1.03

nm) of Pb, an elaborate proof for the QSE requires atomically flat films with precise control of their thicknesses on a macroscopic scale by which the properties can be characterized. Due to the large lattice mismatch and different chemical bonding nature, preparation of a metal film with atomic level precision on a semiconductor substrate remains a great challenge in material science [14, 15].

We have investigated the low-temperature molecular beam epitaxy (MBE) growth of Pb thin films on Si (111) surfaces, and have successfully prepared atomically flat Pb films with known absolute thicknesses in terms of atomic layers. The QSE is systematically studied by measuring the thickness-dependent growth mode, electronic structure (the density of states near E_F and electron–phonon coupling) and physical properties (superconductivity and thermal expansion) by using reflection high energy electron diffraction (RHEED), STM and ARPES, and a persistent QSE resulted 2 ML oscillation in these quantities is established, as reported here.

2 Experimental results and discussion

2.1 QSE in the STM manipulation of wedge-shaped islands

The experiments were carried out in an ultrahigh vacuum (~5×10^{-11} Torr) variable temperature STM system equipped with a MBE chamber for thin film growth. The Pb islands were grown by depositing high purity (99.999 %) Pb from a Knudsen cell on Si (111) substrates pre-cleaned using standard flashing procedure [16]. During Pb deposition, the Si substrates were held at 145 K with flowing liquid nitrogen. The STM images were taken with a typical tunneling current of ~20 pA and a bias voltage of 1.5 V at both room temperature (RT, 300 K) and low temperature (LT,240 K), while the STM manipulations were executed by applying a voltage pulse of up to 10 V when the scanning tip was located at a place of interest with its feedback active. Right after the pulse, the normal STM scanning was immediately resumed to monitor the morphological evolution.

On a stepped substrate [Fig. 1 (a)], the flat-top Pb (111) islands containing several thicknesses along the ascending of the Si substrate are formed, as illustrated schematically in Fig. 1 (i), where both even and odd layers appear. Because of the special trait of Pb/Si (111), the electronic structure of Pb films change dramatically with a period of about 2 ML. Usually, QSE favors only even layers (more stable), because the energy quantization of internal electrons results in a higher total electron energy in the odd-layered regions (labeled with the red color) than that in even layers (labeled with the blue) in Fig. 1 (i), as indicated by the electron interference fringes on the wedge-shaped island [4]. We anticipate that if 1 ML Pb is added only on the top of those odd-layered regions, every region of the Pb island becomes even-layered [Fig. 1(j)] and hence the system energy is lowered in terms of QSE. However, the QSE is satisfied at the expense of creating additional surface steps, by raising the total surface step free energy. If the two effects are comparable in quantity, the system is frustrated for being unable to satisfy both step energy minimization and QSE. In reality, achieving this dynamic process is very difficult.

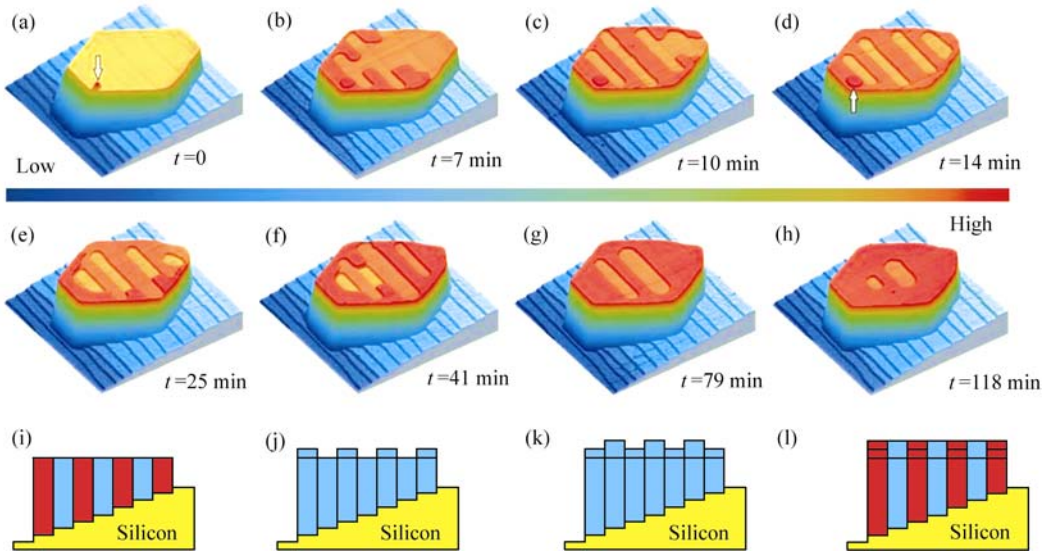

Fig. 1 A sequence of STM images (1000 nm×1000 nm) recorded at room temperature (**a**–**h**), showing the evolution of a wedge-shaped Pb (111) island on Si (111). A voltage pulse of 5 V was applied near the island edge for several milliseconds, as indicated with an arrow in (**a**) for an original island before STM manipulation where the Pb island increases its thickness successively from 4.5 nm to 7.3 nm. The below side-view schematics show: (**i**) initial flat-top Pb island, (**j**) selective strip growth turning odd-layered regions into even-layered (**b**–**d**), (**k**) double-layer strip growth maintaining the even-layered state (**e**–**h**), and (**l**) a flat-top wedge after the growth of two atomic-layers of Pb.

We find that by applying an electrical trigger pulse using an STM on this system, massive atom transport could be initiated in a controllable manner to transform the film morphology and swing the system back and forth between the two extreme states [Fig. 1(i), (j)] favored by each force, adding precisely 1 ML to the island thickness with a full cycle of this nanoscale "free-energy pendulum". This situation is clearly shown by the sequential STM snapshots in Fig. 1, where Fig. 1(a) and (i) show the original flat-top Pb island and its schematic cross-section, respectively. After applying an electrical pulse (5 V) with an STM tip, a new Pb layer begins to grow spontaneously from where the voltage pulse was applied [as indicated by the arrow in Fig. 1 (a)]. The early stage of the pulse-induced growth is characterized by a novel selective strip-flow behavior confined by the Si substrate step edges [Fig. 1 (b–d) and (j)]. As discussed above, one atomic layer grows only on the odd-layered regions, leaving the original even-layered regions unchanged. This strip-flow growth continues until all regions become even layered. Until then, the system has transformed into a new state where quantized electron energy is minimized [Fig. 1 (d) and (j)], while the surface has a stripped configuration. It is clear that the selective strip-flow growth is driven by QSE at the expense of surface step energy. If no additional voltage pulse is applied, the system will recover its flat top geometry seen in Fig. 1 (a) by atom incorporation at the steps to minimize the surface step energy, but now at the expense of raising the quantized electron energy (image not shown). In this way, for each operation one full monolayer of about more than one million Pb atoms is precisely added on the wedge surface.

Such QSE-driven island evolution could also display more intricate dynamics. If we control the manipulation by applying a second pulse just before the recover of the flat top surface, a double-layer strip growth can be achieved and shown in Fig. 1 (e)–(g), and (k). In this case, QSE dominates over the step effects causing a spontaneous bi-layer growth and the system always maintains to satisfy the QSE [17]. Again, when left alone, the growth will ultimately proceed to restore the flat-top configuration [Fig. 1 (g) and (h)].

The most intriguing part of this result is why the system in the quantum regime behaves like a "pendulum", and chooses to swing to the extremes globally rather than to evolve along a compromised pathway. While in the classical regime, where the QSE is not predominantly involved with the film thickness above 20 ML, a manipulation with STM tip will always induced a layer-by-layer mode where the growth begins first with wetting the island's edge followed by the decay of the vacancy island [18]. Our experiments clearly show that with different weight of QSE contributing to the driving forces, different growth dynamics can be realized with a stripe-flow growth mainly due to QSE, or with a layer-by-layer growth characterized with a special growth behavior of vacancy island growth closely related with the classical effects. Particularly in the regime favored by QSE, it is possible to construct the quantum intrinsic structures instead of the classical stable ones [19].

2.2 Novel Growth behavior of Pb films and band structure determination by quantum well spectroscopy

During Pb thin film growth in the MBE chamber, the substrate was cooled to about 145 K by a copper block with two liquid nitrogen vessels. RHEED patterns were used for the real-time monitoring of film growth and were taken along the $[1\bar{1}0]$ azimuth of the Si (111)-7×7 surfaces at glancing incidence angle with an electron beam energy of 12 keV. After growth, the samples were directly transferred to an ultra-high vacuum (5×10^{-11} Torr) analysis chamber, where an Omicron STM and an ARPES system were installed for in situ surface morphology and electronic structure characterization. The photoemission spectra were collected by a GAMMADATA SCIENTA SES-2002 analyzer, with an energy resolution of 2 meV.

2.2.1 The growth behavior of Pb/Si (111)

To achieve an ideal 2D system, we have performed a systematic study of the growth of Pb on Si (111) with a low temperature deposition method [20]. With this method, flat metal films had been prepared on several semiconductor substrates, which exhibit intriguing thickness-dependent stability [20–24]. An "electronic growth" model was used to account for the special growth mode, where QSE plays an important role in the magic stability of thin films [26].

The upper panel in Fig. 2 displays the sequential RHEED patterns during growth at a substrate temperature of 145 K. The 7× fractional diffraction streaks become weak after 1 ML Pb deposition [Fig. 2 (a)] and disappear completely at 1.5 ML (not shown) because of formation of the typical featureless wetting layer. With increasing thickness, 1×like long dim streaks superimposed with bright spots appear [Fig. 2 (b)], suggesting the formation of 3D islands above the wetting layer. The spots, the fingerprint of the 3D islands are interconnected gradually and replaced with long sharp streaks at ~6 ML [Fig. 2 (c)]. Then, a layer-by-layer growth dominates above 6 ML. With further Pb deposition, there is no noticeable change in the RHEED patterns [Fig. 2(d)]. These results are in good agreement with a previous real-time X-ray study [27]. This growth behavior is understandable since 2D growth is kinetically accessible due to decreased atom diffusion at a low temperature compared to the traditional methods where 3D growth is thermodynamically promoted.

The lower panel in Fig. 2 shows the corresponding STM images recorded at room temperature. Below 1.5 ML, the featureless wetting layer, consisting of small Pb clusters, is seen in Fig. 2 (e). Many 3D flat-top islands are observed when the thickness is smaller than 6 ML [Fig. 2(f)], corresponding to the streak-plus-spot RHEED pattern in Fig. 2 (b). Surprisingly, while a uniform film in the thickness regime (6 ML ~10 ML) is expected from the RHEED pattern in Fig. 2 (c), the corresponding room-temperature morphology ex-

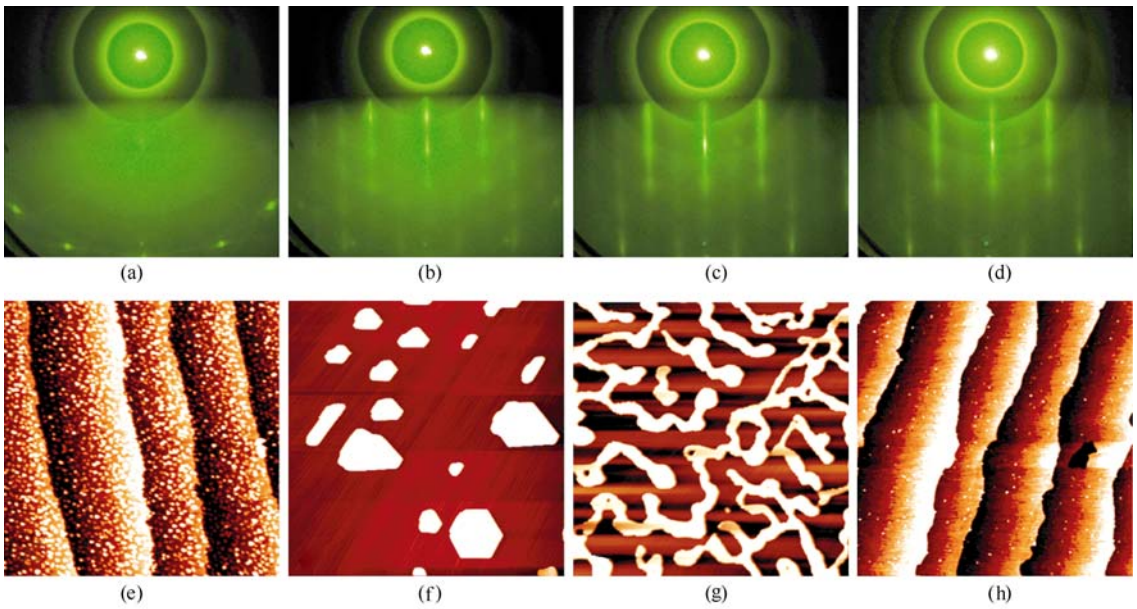

Fig. 2 RHEED patterns (**a**–**d**) taken during Pb deposition on Si (111) substrate at 145 K, and the corresponding room temperature STM images (**e**–**h**). The image size is 2 000 nm×2 000 nm. Nominal thicknesses for the Pb films are 1 ML, 3.5 ML, 6 ML and 10 ML for (a), (b), (c) and (d), respectively.

hibits interconnected islands [Fig. 2 (g)]. The films only become stable at room temperature when the coverage is $\geqslant$10 ML, as shown by the STM image in Fig. 2 (h). Hence, 10 ML can be identified as a critical thickness (or the smallest thickness) for the formation of stable films at room temperature.

The above morphology evolution ($<$10 ML) can be qualitatively explained by the "electronic growth" model. According to this model, the stability of a thin film is intimately related to the electronic contribution to the system energy, which mediates a long-range force, counteracting the unfavorable over-layer substrate interface energy [26]. The trade-off between the energy minimization by the long-range force and the energy punish due to the thermal effects defines a "critical thickness" of 10 ML at room temperature.

Above 10 ML, the growth exhibits another interesting double-layer growth mode (Fig. 3). When the 13 ML film shows an atomically smooth surface [Fig. 3 (a)], the 14 ML film is actually composed of a flat 13 ML film plus 2 ML high islands covering 50 % percent of the surface. Since we can't simply use STM to determine the absolute film thickness, the magic stability or the growth behavior identification demands a more sensitive tool. Photoemission spectroscopy probes the quantized energy levels or the QWS, which can be used to measure indirectly the film thickness by a Bohr-Sommerfeld quantization rule, as reported in previous study [2]. Series ARPES spectra of the Pb films with atomically flat surface are displayed in Fig. 3 (c). The sharp and intense peaks near the Fermi level correspond to the QWS peaks, while the broad and less intense peaks with a binding energy larger than 0.5 eV derives from the resonance states. Evidently, if a film is terminated with a complete layer, its spectra will show only one set of intense and

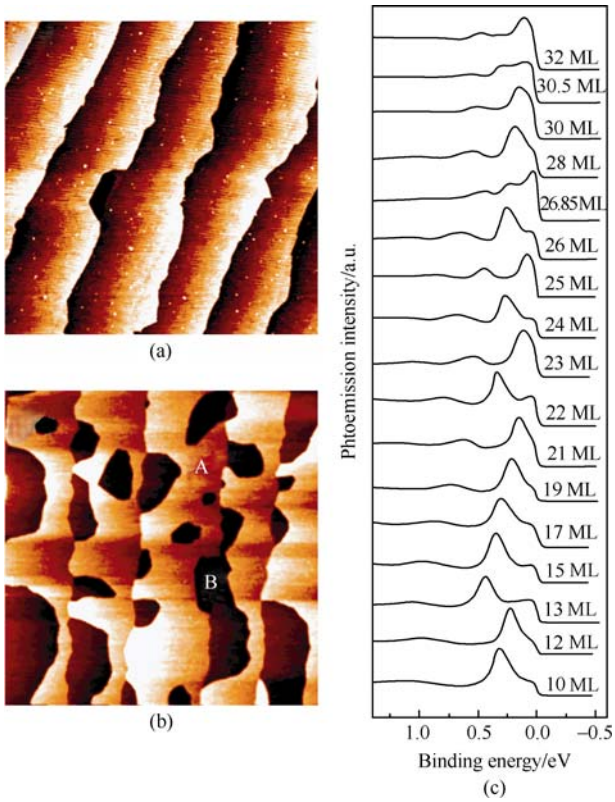

Fig. 3 Room temperature STM images (2 000 nm × 2 000 nm) of the Pb films of 13 ML (**a**) and 14 ML (**b**). All stable films exhibit essentially the same morphology as shown in (**a**), and are (111) oriented. In (**b**), the letter "A" indicates the 2 ML high islands on top of the 13 ML film labeled with the letter "B". (**c**) Normal emission spectra measured at 110 K with the successive spectra graphically offset for clarity. Binding energy at 0.0 eV corresponds to the Fermi level.

sharp QWS peaks. Such spectra were observed for the stable films of 10 ML, 12 ML, 13 ML, 15 ML, 17 ML, 19 ML, 21 ML, 22 ML, 23 ML and 24 ML. However, for the films with nominal thicknesses of 11 ML, 14 ML, 16 ML, 18 ML and 20 ML where half of the surface is covered by 2 ML-high islands, the corresponding photoemission spectra exhibit a mixture of different sets of QWS peaks from the adjacent stable layers as shown before [26]. Based on the measurement by both ARPES and STM, a double-layer growth mode can be identified between 10 ML and 21 ML with a turning point at 13 ML, where the stable thicknesses change from even layers (below 13 ML) to odd layers. Above 21 ML, the growth proceeds via a quasi layer-by-layer mode and continuous layers could be obtained.

2.2.2 Band structure determination

To understand the magic stability of the Pb films, we did careful analysis of the photoemission data. By fitting the QWS energy with the phase accumulation model, the band structure of Pb was obtained. For s-p metals, the quantized energy levels (or QWS) are often described with the phase accumulation model [2],

$$2k(E)Nd+\phi_s(E)+\phi_i(E)=2\pi n \quad (1)$$

where $k(E)$ is the electron wavevector along the ΓL (111) direction, $\phi_s(E)$ and $\phi_i(E)$ are the phase shifts for an electron upon reflection at the surface and the interface, respectively. n (an integer) is the QWS index, N is the number of atomic layers in the film, and d = 2.8435 Å is the lattice spacing along the ΓL direction [29].

Because the phase shift depends strongly on the electron energy, the wavevector $k(E)$ at a given energy can be calculated with a simple formula,

$$k(E)=\pi(n_2-n_1)/[(N_2-N_1)d] \quad (2)$$

where N_1 and N_2 correspond to the film thicknesses with the same QWS energy (E), and their index is labeled with n_1 and n_2, respectively. $k(E)$ as determined by this method is shown in the insert of Fig. 4 (a), where the QWS energy exhibits an approximately linear dependence on k. Since this energy band comes from band folding from the second Brillouin zone, we fit the band using $E=-\frac{\hbar^2(2k_{Bz}-k_F)}{2m_e^*}(k-k_F)$. The fitting yields an effective electron mass of $m_e^* = 1.2m_e$ (m_e is the free electron mass) and a Fermi wavevector of $k_F = 0.611$ Å^{-1}, or $k_{F'} = 2k_{Bz} - k_F = 1.598$ Å^{-1} before the band folding. This value is very close to the value of 1.596 Å^{-1} obtained from the De Hass-Van Alphen measurement within an extended Brillouin zone scheme [29, 30].

We further fit the QWS energy in the E-d plane [Fig. 4 (a)] by assuming a linear dependence of the total phase shift on energy, i.e., $\phi_s+\phi_i=\pi(a.E+b)$ The fitted result(diamonds) is in good agreement with the experimental results (shadowed squares). The value of $k_F = 0.611$ Å^{-1} leads to a Fermi level crossing of the QWS at every $\Delta N = \pi/(k_F d) = 1.8$, similar to a previous theoretical calculation [31]. This explains our photoemission data in Fig. 3 (c) that the highest occupied QWS above 21 ML oscillates (with respect to E_F) with a nearly 2 ML period. The 2 ML oscillation was found to result in a spectacular oscillation of the superconducting transition temperature, as discussed below [32].

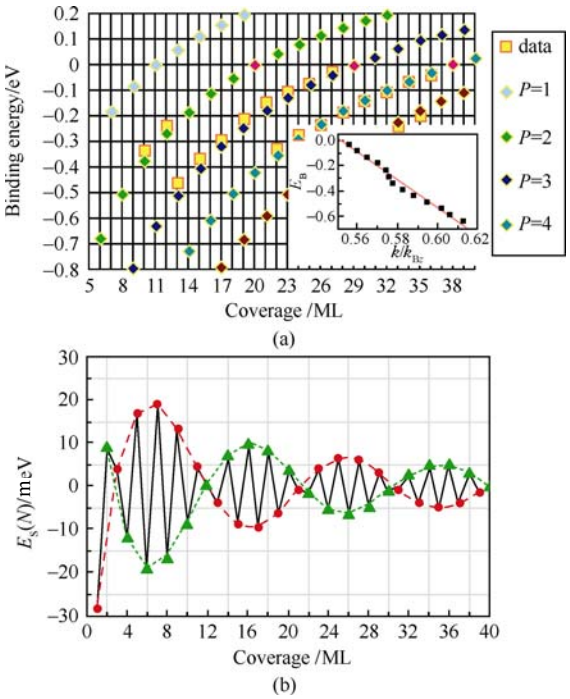

Fig. 4 (**a**) Binding energy of the QWS as a function of Pb film thickness (the shadowed squares and diamonds correspond to the experimental and the fitting results, respectively). For each measured "branch", the reduced quantum member P is indicated in the right panel of the figure. The insert shows the experimental energy band $E(k)$ along the ΓL direction in the first Brillouin zone. (**b**) Calculated relative surface energy as a function of Pb film thickness.

The small difference between $2k_F$ and k_{Bz} generates a "beating effect" with an oscillation period of $\pi/(2k_F - k_{Bz})$ = 9 ML [31], since the thickness of a film is always an integer in terms of the number of atomic layers. In Fig. 4 (a), the QWS labeled with index P (defined as $P \equiv 3N - 2n$) crosses E_F with a 9 ML period. Whenever the QWS of an odd (even) branch P crosses E_F, there will be a switching of the film stability from odd (even) to even (odd) layers. This even-odd switching occurs at 13 ML, 22 ML, and 31 ML, respectively, with an interval of 9 ML. In particular, the films become most unstable if their QWS is right at E_F. This situation appears at 11 ML, 20 ML, 29 ML, and 38 ML, again with an interval of 9 ML.

Based on the "electronic growth" model, we can understand the novel stability of the Pb films. From our experiment, for P=2 (10 ML, 12 ML) and P=3 (13 ML, 15 ML, 17 ML, 19 ML, 21 ML), the occupied QWS of the stable films has a lower energy than the adjacent unstable layers. With increasing film thickness, the energy difference between the odd and even layers becomes smaller, eventually leading to a quasi layer-by-layer growth above 21 ML. Rela-

tive surface energy calculation can provide us a global understanding of the novel stability as a function of film thickness [33]. Based on the experimental results, we calculated the surface energy of the Pb films in a Friedel form [34]:

$$E_s(N) = A\frac{\cos\left[2k_F(N+\Delta N)d\right]}{(N+\Delta N)^{\alpha}} + B \quad (3)$$

where k_F = 1.598 Å^{-1} from our experiment, d =2.8435 Å is the atomic layer spacing, α =0.938, and A and B are constant. ΔN is the additional thickness caused by the quantum well width change associated with the charge transfer between the Pb overlayer and the substrate [9]. As shown in Fig. 4 (b), Eq. (3) represents a damped sinusoidal function with a Friedel oscillation wavelength that is half of the Fermi wavelength (1.8 ML in Pb), riding on an envelope "beating" function with a 9 ML internodes distance. The film stability and the growth behavior observed in our experiments are consistent with this calculation.

Clearly, the stability of the Pb films is closely related to the electronic structure or the formation of the QWS, thus is modulated by the QSE. The new result here is the dramatic manifestation of the persistent QSE on the film stability up to 21 ML. A one-to-one correspondence between the film stability and the electronic structure is established. Many intrinsic traits, such as both the 2 ML and the 9 ML oscillation periods in film stability and in electronic structure, are also identified. The determination of the band structure, the Fermi wavevector and the effective mass provides more profound understanding of this system [35].

2.3 Quantum oscillation of superconductivity

Because of the progressing of energy as a function of film thickness and the discrete nature of QWS, the position of the highest occupied QWS oscillates with respect to E_F (0.0 eV) between the odd and even layers with a 2 ML period. Our first-principles calculations also show a similar feature in the electron density of states at E_F [36]. Since many physical properties such as superconductivity depend strongly on the distribution of electrons near E_F, we anticipate a similar oscillatory behavior in the superconductivity of Pb films. The influence of QSE on the superconductivity of thin films is a topic of fundamental importance in solid state physics, and the internal idea was discussed early in the 1960s [37]. According to the theory, the superconducting transition temperature decreases as the thickness is decreased [38, 39]. Non-monotonic behavior in superconducting transition temperature was reported experimentally previously, since the samples were not structurally defined and exhibit typical polycrystalline and granular morphology [40–42]. However, a convincing proof for QSE on the superconducting transition is the quantum oscillation.

The atomically uniform thin films over a macroscopic area enables us to observe this quantum oscillation. The ex situ transport measurements of the Pb films covered by ~4 ML Au were performed with a quantum design magnetic property measurement system (MPMS-5). From the temperature dependence of the film resistance, the superconducting transition temperature (T_c) is defined as the temperature at which the film resistance becomes half of the normal state resistance at T = 8 K, as indicated by the arrow in the insert of Fig. 5. The transition temperature (black solid balls) as a function of film thickness is plotted in Fig. 5, where an overall trend of increasing T_c with increasing film thickness is seen which is consistent with the feature of conventional two-dimensional superconductors. An oscillatory behavior in T_c is clearly observed with a period of 2 ML for films above 21 ML: a higher T_c for the even number thicknesses and a lower T_c for the odd number thicknesses. Monotonic behavior in T_c below 21 ML is also noticed because of the missing intervening even layers. One can easily imagine an oscillatory behavior if these even layers could be created.

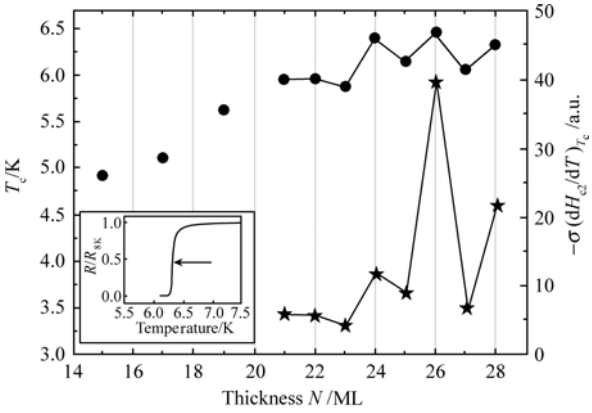

Fig. 5 Superconducting transition temperature T_c (*dots*) and density of states $N(E_F) \propto -\sigma(dH_{c2}/dT)_{T_c}$ (*stars*) plotted as a function of Pb film thickness, clearly demonstrating an non-monotonic oscillatory behavior in both T_c and $N(E_F)$. The insert shows the resistance as a function of temperature measured from the 28 ML film, which reveals a sharp transition to superconductivity at 6.32 K, as indicated by the arrow.

According to the Bardeen-Cooper-Schrieffer (BCS) theory of superconductivity [43], T_c depends exponentially on the density of states at E_F and on the electron-phonon coupling, which mediates the binding of Cooper pairs in the form of:

$$k_B T_c = 1.14\hbar\omega_D \exp\left[-1/N(E_F)V\right] \quad (4)$$

where k_B is the Boltzmann constant, ω_D is the Debye frequency, $N(E_F)$ is the density of states per spin, and V is the phonon-mediated attractive interaction at the Fermi surface. For a system with the QSE involved, $N(E_F)$ oscillates with t as $N(E_F) = (m^*/\pi\hbar^2 t)\left[2t/\lambda_F\right]$ and t is the film thickness, where m^* is the effective mass of electrons, $\hbar$ is the Planck constant, and $\left[2t/\lambda_F\right]$ is the integer part of $2t/\lambda_F$. With this simple description, an oscillating T_c with a period of 4 Å in Sn films was interpreted to be due to the QSE [40]. In our case, the λ_F of Pb is nearly 4 ML, this is why the oscillating period is 2 ML.

In situ measurement of the electron density of states was

also executed to understand the origin of the oscillatory T_c. The photoemission data in Fig. 3 (c) cannot be directly used for two reasons. Firstly, those data were collected along the normal-emission direction (perpendicular to the sample surface), which is not a complete measurement of the density of states. Secondly, those data were obtained in situ for the bare Pb films without the Au overlayers. An independent estimation of $N(E_F)$ was done by measuring the film resistance (R) as a function of applied magnetic field (H) along the surface normal direction at different temperatures near T_c separately, namely the R-H curve from which the H_{c2}-T curve is estimated. Here, H_{c2} is the upper critical field, defined as the magnetic field at which the film resistance R reaches to half of the normal state resistance at the onset point for superconducting transition. In the Ginzburg-Lan- dau-Abricosov-Gorkov theory, the $N(E_F)$ of a Pb film is proportional to the slope dH_{c2}/dT of the upper critical field near T_c via [44],

$$N(E_F) \propto -\delta\,(dH_{c2}/dT)_{T_c} \tag{5}$$

where δ is the normal state conductivity. The relative conductance δ was estimated from the sample size. The fitting result for dH_{c2}/dT from the measurement is plotted in Fig. 5 (stars), which clearly shows a nice correspondence between the density of states and T_c [32].

2.4 Quantum oscillation of electron-phonon coupling and thermal expansion coefficient

In this part, variable temperature ARPES measurement was carried out to determine the electron-phonon coupling and thermal expansion. A sample manipulator with a button heater attached to the head of an open-cycle He cryostat flowed with liquid nitrogen, was used to control the substrate temperature from 20 K to 300 K with a precision of ±0.1 K during ARPES measurement.

2.4.1 Quantum oscillation of electron phonon coupling strength

As shown above, the electron density of states at the Fermi energy is not the only factor affecting the superconducting transition temperature. For a conventional superconductor such as Pb, electron-electron attraction necessary for the binding of Cooper pairs is ultimately due to electron-phonon interactions [45]. As we mentioned earlier, the formation of QWS strongly regulates the mechanical stability of films reflected with expansion and shrinkage of interlayer spacing [46]. Both of the factors speak directly to the possibility of modulating the electron-phonon coupling.

Similar to other spectroscopy, the photoemission spectroscopy does not simply probe the ground state, rather, the resulting decayed excitations (the photoholes), and thus many-body effects such as electron-phonon coupling could be involved experimentally. In the last few years, prominent progress has been made in the study of electron-phonon coupling strength (λ) for the surface states in bulk materials [47–49] or for the QWS in thin films by ARPES [50–53]. For crystalline metal surfaces, the observed photoemission peak width is proportional to $\hbar/\tau$, where τ is the lifetime of the hole state excitations. At high temperatures (greater than one-third of the Debye temperature) and small hole energies (lower than the bandwidth), the temperature-dependence of the QWS peak width is actually a good measure of the phonon contribution to the hole lifetime. Since the influence of the electron-electron interactions and the defect scattering are negligible in this case, and the inverse hole lifetime can be given by $\hbar/\tau = 2\pi\lambda k_B T$, where λ equals $2\pi k$ times the slope of the peak width vs. temperature.

The variable temperature ARPES spectra for the 23 ML and 24 ML films are shown in Fig. 6. With increasing substrate temperature, the peak position of the QWS shifts towards higher binding energies while the peak width broadens [54]. To find out the exact relation between the linewidth (ΔE) of the QWS and the temperature, a curve fitting by Voigt profile with Lorentzian line shape was made. Typical fitted results are plotted in Fig. 7 (a) for the films of 22 ML and 23 ML, where ΔE increases linearly with increasing temperature and exhibits prominent different slopes for the adjacent layers. According to the previous discussion, this slope is related to the λ value via

$$\lambda = \frac{1}{2\pi k_B}\frac{d\Delta E}{dT} \tag{6}$$

The λ values derived from the QWS peaks for different film thicknesses are shown in Fig. 7 (b) (triangles), where only the values for stable layers(15, 17, 19, 21, 22, 23, 24 ML)

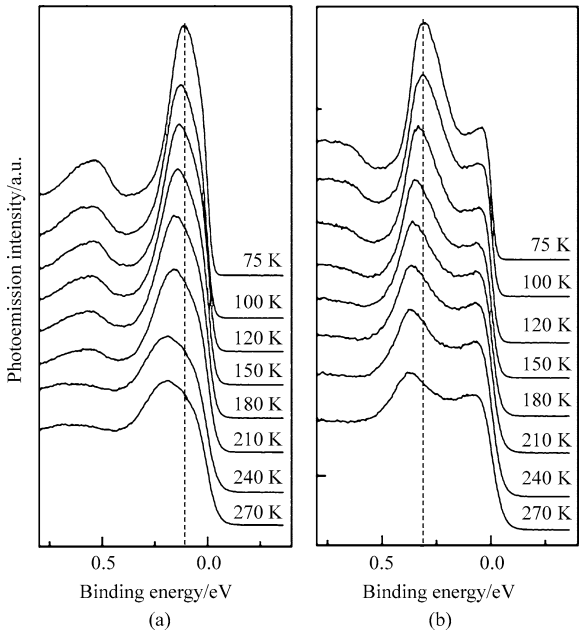

Fig. 6 Temperature-dependent photoemission spectra of Pb films for (**a**) 23 ML and (**b**) 24 ML collected within a temperature range 75–270 K. The vertical dashed lines reveal the variation of the QWS binding energy as the film temperature is changed.

are plotted. Besides an overall gradual increase of the λ towards the bulk value (1.55) [55], an oscillation of λ with a period of 2 ML is clearly noted from 21 to 24 ML. As a comparison, the T_c for the Pb films is also shown in Fig. 7 (b) (dots). A clear correspondenchie between λ and the experimental T_c for different layers is obvious, but the variation trend is inversed in amplitude vs. tckness above 21 ML. That is to say, a larger λ corresponds to a lower T_c. This is because the experimental T_c was acquired with the Pb films covered by 4 ML Au while the photoemission data for the measurement of λ was taken from the clean surfaces.

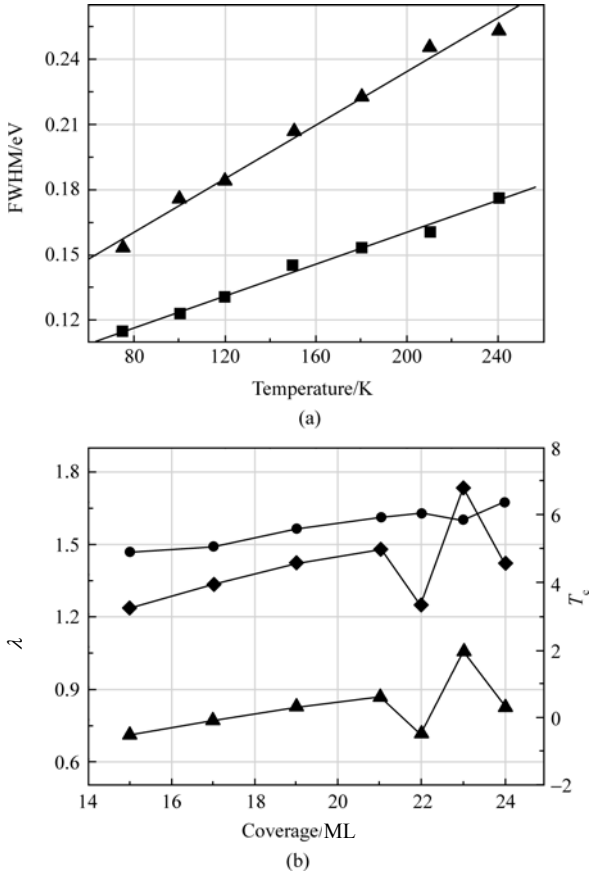

Fig. 7 (**a**) Lorentzian peak widths of the QWS of the 22 ML (*square*) and 23 ML (*triangle*) films plotted as a function of temperature. (**b**) Measured λ (*triangles*) and calculated superconductivity transition temperature (*diamonds*) by the formula $T_c = \frac{\Theta_D}{1.45}\exp\left[-\frac{1.04(1+\lambda)}{\lambda-\mu^*-0.62\lambda\mu^*}\right]$ as a function of thickness. In the calculation, typical values of 0.1 for μ^* (the effective Coulomb interaction) and 105 K for Θ_D (the Debye temperature) were used. As a comparison, the experimental transition temperature of the Pb films is also displayed (*dots*).

2.4.2 Quantum oscillation of the thermal expansion coefficient

Another important result in Fig. 6 is that, for both films, the QWS peaks shift always towards higher binding energies with increasing substrate temperature. For all Pb films studied in this work, the maximum shift of the QWS binding energy is less than 100 meV when the temperature varies from 75 K to 270 K. For example, the net shifts for the films of 23 ML and 24 ML are 84 meV and 65 meV, respectively.

Such thermal-induced shift in QWS energy was observed in Ag/V (100) and Ag/Fe (100) systems previously [52, 56], but opposite results were obtained: the binding energy increases in Ag/V (100), and it decreases in Ag/Fe (100) with increasing temperature. Our result is similar to that in Ag/V (100). Three factors cause the shift of the QWS energy with the thermal effects: the width of the potential well, the Fermi level, and the phase shift at the interface. For a 2D system, change of the phase shift at the interface plays minor effect [57].

To quantify our experimental results, the temperature-dependence of the QWS binding energy for some Pb films is fitted linearly and shown in Fig. 8 (a). We attribute the shift of the QWS energy to the thermal broadening of the confinement well width, as well as the variation of the Fermi level of the films. Within a free electron approximation, the temperature-dependence of the Fermi energy of a bulk material is described as,

$$dE_F / dT = -2E_F\alpha_r \tag{7}$$

where α_r is the linear thermal expansion coefficient of the material, and E_F is its Fermi energy calculated relative to the bottom of the valence band (for bulk Pb, E_F =9.47 eV). The thermal shift of the QWS energy (E_{QW}) with respect to the bottom of valence band has a form of:

$$dE_{QW} / dT = -2E_{QW}\alpha_z \tag{8}$$

where α_z is the linear expansion coefficient along the confined direction. For thin film, its linear expansion in the film plane (*x*-*y* plane) should be very close to that of bulk Si. While in the *z* direction, because of the Poisson effects and that the linear expansion coefficient of Si (2.8×10^{-6} K^{-1}) is one order of magnitude lower than that of Pb (2.89×10^{-5} K^{-1}), the thermal expansion is expected to be larger than that of bulk Pb. This results in an increase of the QWS binding energy as the temperature is increased. We calculated the linear thermal expansion coefficient [Fig. 8 (c)] along the confined direction by using the experimental thermal shift of the QWS energies with Eqs. (7) and (8). Several observations can be made: (1) the calculated thermal expansion coefficients in the film normal direction are greatly enhanced than that of bulk Pb; (2) the overall trend is that a lower value corresponds to a film with a higher QWS binding energy; (3) a 2 ML oscillation behavior appears from 21 ML to 24 ML.

To understand the global enhancement of the linear thermal expansion coefficient, we use α_r, α_P and α_z to describe the linear expansion coefficient of free standing film, the confined film in the film plane and the film normal direction, respectively. α_z can be expressed as,

$$\alpha_z = \alpha_r + \frac{2(\alpha_r - \alpha_P)\eta}{1-\eta} \tag{9}$$

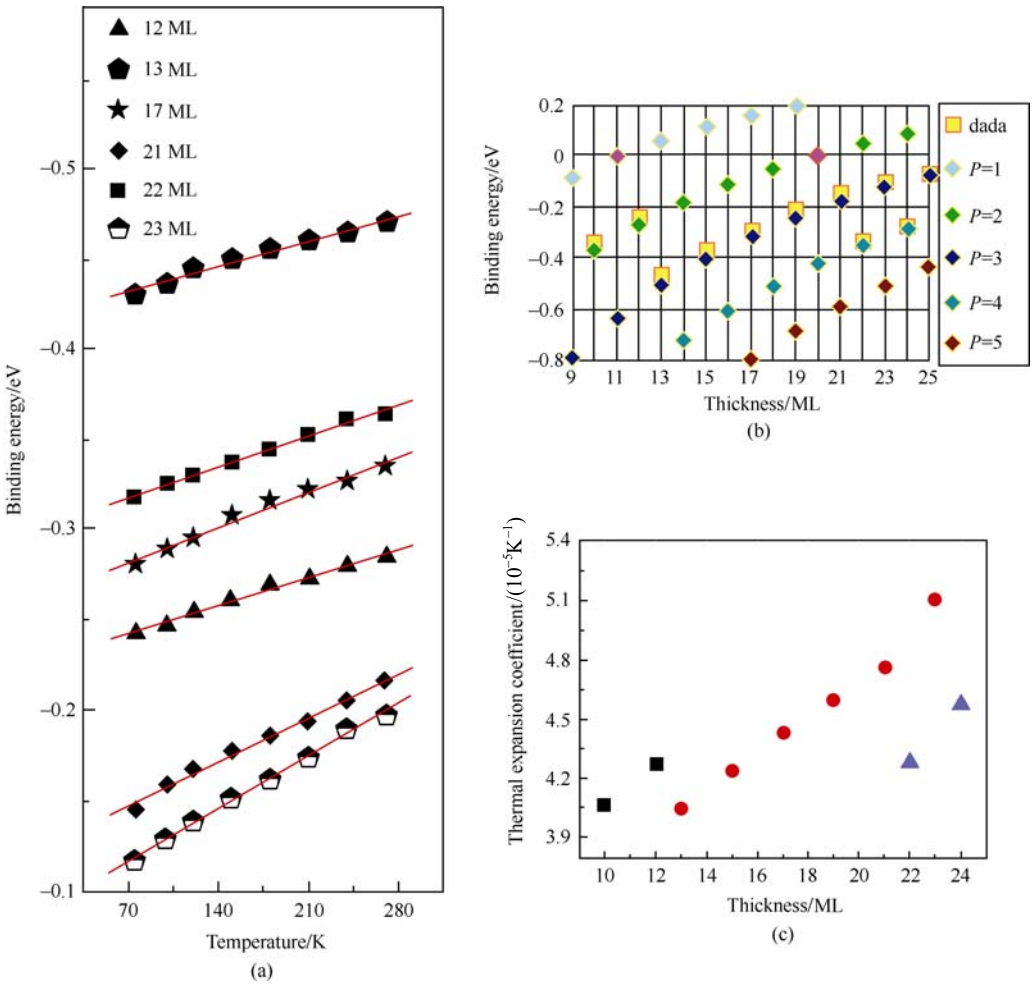

Fig. 8 (**a**) Binding energy of the QWS plotted as a function of temperature. The dots and lines indicate the experimental data and linear fits, respectively. (**b**) Experimental QWS binding energy (*squares*) and theoretical values fitted within a one dimensional square well model (*diamonds*) in terms of atomic layers. (**c**) Thermal expansion coefficients of the Pb films along the confined direction calculated with the proposed model.

where η is the Poisson ratio. For Pb/Si (111), substituting α_r and α_P by the linear expansion coefficients of bulk Pb and bulk Si, respectively, and taking η as the Poisson ratio of bulk Pb (0.44), we obtain that α_z equals 2.414 α_r. Namely, in an ideal case, the thermal expansion in z direction should be enhanced by a factor of two compared to the bulk, which is adequate to explain the global enhancement of our experimental data. A more straightforward explanation of this oscillatory thermal expansion coefficient can refer to the so-called misfit function [58, 59]:

$$\delta(n) = \left| nd_0 - m\frac{\lambda_F}{2} \right| \tag{10}$$

where n is the number of atomic layers, and m is an integer and selected to make δ a minimum. Generally speaking, a dramatic mismatch with a large δ can make the electron standing waves not fit properly into the potential well (nd_0). This corresponds to a lower QWS binding energy and a less stable film. On the contrary, a lower δ implies a well matched system and a stable film with higher QWS binding energy.

The prominent difference of the expansion behavior between the even and the odd Pb layers should be a manifestation of different film stability. It is obvious that a large expansion coefficient can be expected for an unstable film with a large δ. For the films of 21 ML or 23 ML thick, δ is close to $\lambda_F/4$ (its maximum value). In this case, further change (either decrease or increase) of the confinement well width will decrease the mismatch and the system energy, and expansion will become easier. On the other hand, for a stable layer (22 ML or 24 ML) with a small δ (close to 0), expansion will increase the mismatch between nd_0 and $m\lambda_F/2$, thus the expansion in these films is more energetically unfavorable. As shown previously [28], the film stability oscillating with a period of 2 ML is interpreted to be due to the formation of the QWS, so does the thermal expansion coefficient [60].

3 Conclusions

We have performed a systematic investigation of the QSE in Pb/Si (111) system by using two different types of samples. We demonstrate a dynamic morphology evolution process caused by the competition between QSE and classical effects in the Pb islands manipulated by an STM tip. By preparing atomically flat Pb films with accurate control of their thickness, oscillatory superconducting transition temperature, electron-phonon coupling constant and thermal expansion coefficient were observed. These oscillatory behaviors prove to be directly related to the formation of QWS that greatly modulate the electronic structure near the Fermi level. The influence of QSE on the perpendicular upper critical field, chemical adsorption, as well as the adhesion coefficient in this system has also been studied and will be reported elsewhere [61–63].

Acknowledgements The work was financially supported by the National Natural Science Foundation and Ministry of Science and Technology of China.

References

1. Paggel J. -J., Miller T., and Chiang T. -C., Quantum-well states as Fabry-Pérot modes in a thin-film electron interferometer, Science., 1999, 283: 1709–1711
2. Chiang T. -C., Photoemission studies of quantum well states in thin films, Surf. Sci. Rep., 2000, 39: 181–235
3. Milum M., Pervan P., and Woodruff D. -P., Quantum well structures in thin metal films: simple model physics in reality, Rep. Prog. Phys., 2002, 65: 99–141
4. Altfeder I. -B., Matveev K. -A., and Chen D. -M., Electron fringes on a quantum Wedge, Phys. Rev. Lett., 1997, 78: 2815–2818
5. Su W. -B., Chang S. -H., Jian W. -B., Chang C. -S., Chen L. -J., and Tsong T. -T., Correlation between quantized electronic states and oscillatory thickness relaxations of 2D Pb islands on Si (111)-(7×7) Surfaces, Phys. Rev. Lett., 2001, 86: 5116–5119
6. Yeh V., Berbil-Bautista L., Wang C. -Z., Ho K. -M., and Tringides M. -C., Role of the metal/semiconductor interface in quantum size effects: Pb /Si(111), Phys. Rev. Lett., 2000, 85: 5158–5161
7. Hupalo M. and Tringides M. -C., Correlation between height selection and electronic structure of the
8.
9. uniform height Pb/Si (111) islands, Phys. Rev. B., 2002, 65: 115406 (1–4)
10. Budde K., Abram E., Yeh V., and Tringides M. -C., Uniform, self-organized, seven-step height Pb/Si(111)-(7×7) islands at low temperatures, Phys. Rev. B., 2000, 61: R10602–R10605
11. Czoschke P., Hong Hawoong., Basile L., and Chiang T. -C., Quantum oscillations in the layer structure of thin metal films, Phys. Rev. Lett., 2003, 91: 226801(1–4)
12. Upton M. -H., Wei C.-M., Chou M. -Y., Miller T., and Chiang T. -C., Thermal stability and electronic structure of atomically uniform Pb films on Si(111), Phys. Rev. Lett., 2004, 93: 026802 (1–4)
13. Mans A., Dil J. -H., Ettema A. R. H. F., and Weitering H. -H., Quantum electronic stability and spectroscopy of ultrathin Pb films on Si(111)7×7, Phys. Rev. B., 2002, 66: 195410 (1–7)
14. Jalîochowski M. and Bauer E., Resistance oscillations and crossover in ultrathin gold films, Phys. Rev. B., 1988, 37: 8622–8626
15. Jalochowski M., Hoffman M., and Bauer E., Quantized hall effect in ultrathin metallic films, Phys. Rev. Lett., 1996, 76: 4227–4229
16. Walz J., Greuer A., Wedler G., Hesjedal T., Chilla E., and Koch R., Stress and relief of misfit strain of Ge/Si (111), Appl. Phys. Lett., 1998, 73: 2579–2581
17. Grossmann A., Erley W., Hannon J. -B., and Ibach H., Giant surface stress in heteroepitaxial films: invalidation of a classical rule in epitaxy, Phys. Rev. Lett., 1996, 77: 127–130
18. Li J. -L., Jia J. -F., Liang X. -J, Liu X., Wang J. -Z., Xue Q. -K., Li Z. -Q., Tse J. -S., Zhang Z., and Zhang S. -B., Spontaneous assembly of perfectly ordered identical-size nanocluster arrays, Phys. Rev. Lett., 2002, 88: 066101(1–4)
19. Okamoto H., Chen D. -M., and Yamada T., Competing classical and quantum effects in shape relaxation of a metallic island, Phys. Rev. Lett., 2002, 89: 256101(1–4)
20. Jiang C. -S., Li, S. -C., Yu H. -B., Eom D., Wang X. -D., Ebert Ph., Jia J. -F., Xue Q. -K., and Shih C. -K., Building Pb nanomesas with atomic-layer-precision, Phys. Rev. Lett., 2004, 92: 106104 (1–4)
21. Li S. -C., Jia J. -F., Zhang Y. -F., Liu F.,. and Xue Q. -K, Phys. Rev. B (submmitted)
22. Smith Arthur R., Chao K. -J., Niu Q., and Shih C. -K, Formation of atomically flat silver films on GaAs with a "silver mean" quasi periodicity, Science., 1996, 273: 226–228
23. Huang L., Chey S. -J., and Weaver J. -H., Metastable structures and critical thicknesses: Ag on Si(111)-7×7, Surf. Sci., 1998, 416: L1101-L1106
24. Gavioli L., Kimberlin K. -R., Tringides M. -C., Wendelken J. -F., and Zhang Z. -Y., Novel growth of Ag islands on Si(111): plateaus with a singular height, Phys. Rev. Lett., 1999, 82: 129–132
25. Jiang C. -S., Yu H. -B, Shih C. -K., and Ebert Ph., Effect of the Si substrate structure on the growth of two-dimensional thin Ag films, Surf. Sci., 2002, 518: 63–71
26. Liu H., Zhang Y. -F., Wang D. -Y., Pan M. -H., Jia J. -F., and Xue Q. -K., Two-dimensional growth of Al films on Si(1 1 1)-7 × 7 at low-temperature, Surf. Sci., 2004, 571: 5–11
27. Zhang Z. -Y, Quantum stability of ultrathin metal overlayers on semiconductor substrates, Surf. Sci., 2004, 571: 1–4
28. Zhang Z. -Y., Niu Q., and Shih C. -K., "Electronic growth" of metallic overlayers on semiconductor substrates, Phys. Rev. Lett., 1998, 80: 5381–5384
29. Hong Hawoong., Wei C. -M., Chou M. -Y., Wu Z., Basile L., Chen H., Holt M., and Chiang T. -C., Alternating layer and island growth of Pb on Si by spontaneous quantum phase separation, Phys. Rev. lett., 2003, 90: 076104(1–4)
30. Zhang Y. -F., Jia J. -F, Han T. -Z, Tang Z., Ma X. -C, and Xue Q. -K, Growth, stability and morphology evolution of Pb films on Si(111) prepared at low temperature, Surf. Sci., 2005, 596: L331–L338
31. Anderson J. -R., and Gould A. -V., Fermi Surface, pseudopotential coefficients, and spin-orbit coupling in lead, Phys. Rev., 1965, 139: A1459–A1481
32. Jalochowski M., Knoppe H., Lilienkamp G., and Bauer E., Photoemission from ultrathin metallic films: quantum size effect, electron scattering, and film structure, Phys. Rev. B., 1992, 46: 4693–4701

33. Wei C. -M. and Chou M. -Y., Theory of quantum size effects in thin Pb(111) films, Phys. Rev. B., 2002, 66: 233408(1–4)
34. Guo Y., Zhang Y. -F., Bao X. -Y., Han T. -Z, Tang Z., Zhang L. -X., Zhu W. -G., Wang E. -G., Niu Q., Qiu Z. -Q., Jia J. -F., Zhao Z. -X., and Xue Q. -K., Superconductivity modulated by quantum size effects, Science, 2004, 306: 1915–1917
35. Boettger J. -C., Smith J. -R., Birkenheuer U., Rosch N., Trickey S. -B., Sabin J. -R., and Apell S. -P., Extracting convergent surface formation energies from. slab calculations, J. Phys: Condens. Matter., 1998, 10: 893–894
36. Czoschke P., Hong Hawoong., Basile L., and Chiang T. -C., Quantum beating patterns observed in the energetic of Pb film nanostructures, Phys. Rev. Lett., 2004, 93: 036103 (1–4)
37. Zhang Y. -F., Jia J. -F., Han T. -Z., Tang Z., Shen Q. -T, Guo Y., and Xue Q. -K., Band structure and oscillatory electron-phonon coupling of Pb thin films determined by atomic-layer-resolved quantum well states, Phys. Rev. Lett., 2005, 95: 096802 (1–4)
38. Zhu W. G. et al. (unpublished data)
39. Blatt J. -M. and Thompson C. -J., Shape resonances in superconducting thin films, Phys. Rev. Lett., 1963, 10: 332–334
40. Haviland D. -B., Liu Y., and Goldman A. -M., Onset of superconductivity in the two-dimensional limit, Phys. Rev. Lett., 1989, 62: 2180–2183
41. Jaeger H. -M., Haviland D. -B., Orr B. -G., and Goldman A. -M., Onset of superconductivity in ultrathin granular metal films, Phys. Rev. B., 1989, 40: 182–196
42. Orr B. -G., Jaeger H. -M., and Goldman A. -M., Transition-temperature oscillations in thin superconducting films, Phys. Rev. Lett., 1984, 53: 2046–2049
43. Paskin A. and Strongin M., Comment on ‘‘transition-temperature oscillations in thin superconducting films’’, Phys. Rev. Lett., 1985, 55: 139
44. Frydman A., The superconductor insulator transition in systems of ultrasmall grains, Physica C., 2003, 391: 189–195
45. Bardeen J., Cooper L. -N., and Schrieffer J. -R., Theory of superconductivity, Phys. Rev., 1957, 108: 1175–1204
46. Sadovskii M. -V., Superconductivity and localization (World Scientific Publishing, Singapore), 2000, 128
47. Allen B. and Dynes R. -C., Transition temperature of strong-coupled superconductors reanalyzed, Phys. Rev. B., 1975, 12: 905–922
48. Crottini A., Cvetko D., Floreano L., Gotter R., Morgante A., and Tommasini F., Step height oscillations during layer-by-layer growth of Pb on Ge(001), Phys. Rev. Lett., 1997, 79: 1527–1530
49. McDougall B. -A., Balasubramanian T., and Jensen E., Phonon contribution to quasiparticle lifetimes in Cu measured by angle-resolved photoemission, Phys. Rev. B., 1995, 51: 13891–13894
50. Balasubramanian T., Jensen E., Wu X. -L., abd Hulbert S.-L., Large value of the electron-phonon coupling parameter (λ=1.15) and the possibility of surface superconductivity at the Be(0001) surface, Phys. Rev. B., 1998, 57: R6866–R6869
51. Hofmann P., Cai Y. -Q., Grütter C., and Bilgram J. -H.., Electron-lattice interaction on α-Ga(010), Phys. Rev. Lett., 1998, 81: 1670–1673
52. Takahashi K., Tanaka A., Sasaki H., Gondo W., Suzuki S., and Sato S., Temperature-dependent angle-resolved photoemission study for quantum-well states in Ag nanofilms, Phys. Rev. B., 1999, 60: 8748–8752
53. Rotenberg E., Schaefer J., and Kevan S. -D., Coupling between adsorbate vibrations and an electronic surface state, Phys. Rev. Lett., 2000, 84: 2925–2928
54. Kralj M., Siber A., Pervan P., Milun M., Valla T., Jonson P. -D., and Woodruff D. -P., Temperature dependence of photoemission from quantum-well states in moving surface vacuum barrier effects Ag/V(100), Phys. Rev B., 2001, 64: 085411 (1–9)
55. Luh D. -A., Miller T., Paggel J. -J., and Chiang T. -C., Large electron-phonon coupling at an interface, Phys. Rev. Lett., 2002, 88: 256802(1–4)
56. Zhang Y. -F, Jia J. -F., Han T. -Z, Tang Z., Shen Q. -T, Guo Y., and Xue Q. -K., Oscillatory electron-phonon coupling in Pb/Si(111) deduced by temperature-dependent quantum well states, Chin. Phys., 2005, 14: 1910–1914
57. Carbotte J. -P., Properties of boson-exchange superconductors, Rev. Mod. Phys., 1990, 62: 1027–1157
58. Paggel J. -J., Miller T., and Chiang T. -C., Temperature dependent complex band structure and electron-phonon coupling in Ag, Phys. Rev. Lett., 1999, 83: 1415–1418
59. Paniago R., Matzdorf R., Meister G., and Goldmann A., Temperature dependence of Shockley-type surface energy bands on Cu(111), Ag(111) and Au(111) , Surf. Sci., 1995, 336: 113–122
60. Hinch B. -J., Koziol C., Toennies J. -P., and Zhang G.., Europhys. Lett., 1989, 10: 341–346
61. Hinch B. -J., Koziol C., Toennies J. -P., and Zhang G.., Single and double layer growth mechanisms induced by quantum size effects in Pb films deposited on Cu(111), Vacuum., 1991, 42: 309–311
62. Zhang Y. -F., Jia J. -F., Tang Z., Han T. -Z., Shen Q. -T., Guo Y., Ma X. -C., Xue Q. -K, Kun X., and Wu S. -C., Thermal expansion enhancement and oscillation of Pb thin films modulated by quantum size effects, Phys. Rev. B (submitted)
63. Bao X. -Y., Zhang Y. -F., Wang Y. -P, Jia J. -F., Xue Q. -K., Xie X. -C., and Zhao Z. -X., Quantum size effects on the perpendicular upper critical field in ultrathin lead films, Phys. Rev. Lett., 2005, 95: 247005 (1–4)
64. Ma X. -C, Jiang P., et al., Direct observation of quantum oscillation of surface chemical activities, Phys. Rev. Lett., 2006 (submitted)
65. Han T. -Z., Jia J. -F., et al. (unpublished data)